Solar Energy Materials & Solar Cells 92 (2008) 1037–1042

Contents lists available at ScienceDirect

Solar Energy Materials & Solar Cells

journal homepage: www.elsevier.com/locate/solmat

Experimental studies and limitations of the light trapping and optical losses in microcrystalline silicon solar cells

Michael Berginski [a,*], Jürgen Hüpkes [a], Aad Gordijn [a], Wilfried Reetz [a], Timo Wätjen [a], Bernd Rech [b], Matthias Wuttig [c]

[a] IEF5-Photovoltaik, Forschungszentrum Jülich GmbH, D-52425 Jülich, Germany
[b] Department of Silicon Photovoltaics (SE 1), Hahn-Meitner-Institut Berlin GmbH, D-12489 Berlin, Germany
[c] Institute of Physics (IA), RWTH Aachen University, D-52056 Aachen, Germany

ARTICLE INFO

Article history:
Received 19 December 2007
Received in revised form
4 March 2008
Accepted 4 March 2008
Available online 29 April 2008

Keywords:
Thin-film silicon solar cells
Light trapping
Optical losses
Quantum efficiency
Limitations

ABSTRACT

This study addresses the potential of different approaches to improve the generated current in silicon thin-film solar cells and modules. Decreasing the carrier concentration in the front contact has proven to increase the quantum efficiency and the cell-current density significantly. Additionally, an optically improved ZnO/Ag back reflector and the optimized light incoupling by anti-reflection layers were studied. In this contribution, we show the potential of the different optical components and discuss combinations thereof in order to obtain a maximized cell-current density in silicon thin-film solar cells. Limitations of the cell-current density are discussed with respect to theoretical calculations.

1. Introduction

Silicon thin-film solar cells are promising candidates for future photovoltaic power generation [1,2]. One approach employs hydrogenated amorphous silicon (a-Si:H)-based active layers in single- or multi-junction solar cells [3,4]. In superstrate configuration, the cell is illuminated through a transparent conductive oxide (TCO) on which the silicon-based p–i–n structure is deposited. Due to the intrinsically low absorbance of silicon in the long-wavelength range, photon management is essential. The photon management comprises efficient coupling of light into the device as well as light trapping within the device. In general, the light trapping is achieved by combining the effective light scattering of the front-contact TCO with highly reflective back contacts. This is an important way to enhance the light-path length within the silicon absorber layer. There are still significant losses, however, due to primary reflection of the light caused by refractive-index mismatch and parasitic absorption in the front-contact TCO, doped layers and back contact. In this contribution, we study the significance of different optical improvements based on experimental data. The influence of the front-contact parasitic absorption, the refractive-index matching at the front contact, as well as an optically improved back reflector are studied in detail in microcrystalline silicon (μc-Si:H) solar cells with intrinsic silicon thickness of 1 μm. The experimentally achieved quantum efficiency is compared to calculations based on theoretical models, especially based on the work of Deckman and Wronski [5]. The expected significance for further optical improvements is estimated by employing the theory of Deckman and Wronski. Finally, this model is used to determine the potential of cell-current density by combining different optical improvements.

2. Experimental

ZnO:Al films were prepared on Corning 1737 glass by rf-magnetron sputtering from ceramic ZnO:Al_2O_3 target with 1 and 0.5 wt% Al_2O_3, respectively. The approximately 800 nm thick, initially smooth films (root mean square (RMS) roughness less than 15 nm) became surface-textured with typical RMS roughness of more than 125 nm by wet-chemical etching in diluted hydrochloric acid (0.5% HCl). For refractive-index matching between front contact and silicon, an additional titanium dioxide (TiO_2) layer with thickness of 50 nm was sputter deposited onto the etched ZnO:Al film. A very thin (10 nm) ZnO layer was applied to protect the TiO_2 from reduction in hydrogen-rich plasma during silicon preparation [6]. The back reflector was improved optically

* Corresponding author at: Schott Solar GmbH, Hermann-Oberth Str. 11, 85640, Putzbrunn, Bavaria, Germany. Tel.: +49 894 62 64153; fax: +49 894 62 64209.
E-mail addresses: Berginski@googlemail.com, berginski@gmx.de (M. Berginski).

0927-0248/$ - see front matter © 2008 Elsevier B.V. All rights reserved.
doi:10.1016/j.solmat.2008.03.005

by introduction of an evaporated SiO_2 layer with a thickness of 50 nm between back-contact ZnO and evaporated silver. The light-trapping ability of a specific TCO film was characterized by application in solar cells. μc-Si:H layers were prepared using plasma-enhanced chemical vapor deposition at an excitation frequency of 13.56 MHz in a $30 \times 30\,cm^2$ reactor. Details of film preparation and characterization are given elsewhere [3,7–9]. Usually, double layers of sputter-deposited ZnO:Al (80 nm) and thermally evaporated silver (700 nm) served as back reflector and rear-side contact. Optical absorption of the layers was measured by photothermal deflection spectroscopy [10] and in air with a dual-beam spectrometer. The solar cell *I*/*V*-characteristics were investigated using a solar simulator (Wacom WXS-140S-Super) at standard test conditions (AM 1.5, $100\,mW/cm^2$, 25 °C). The external quantum efficiency (QE) of the solar cells was calculated from spectral response measured at zero bias. The integrated short-circuit current density was determined using this QE curve employing the AM 1.5 solar spectrum. Henceforth, this calculated current density is referred to as cell-current density j_{QE}. The spectral response measurements were highly reproducible. Thus, the calculated cell-current density j_{QE} exhibited a measurement-reproducibility error of only ±1%.

In the literature, many different approaches have been proposed to derive light-trapping limits from theoretical calculations. Following a statistical mechanical consideration, Yablonovitch and Cody derived a factor of $2n^2$ as the upper limit for light intensity enhancement in a transparent dielectric medium with refractive index n [11,12]. Based on this model, Tiedje et al. presented an extended theory which is much more applicable for solar cells, since the authors also consider a small amount of absorption ($\alpha d < 1$, with α and d being the absorption coefficient and thickness, respectively) in the dielectric medium [13]. The absorption in the dielectric medium is given by

$$A_{\text{Tiedje}} = \frac{\alpha}{\alpha + (4n^2 d)^{-1}}. \quad (1)$$

The corresponding derivation assumes that wave optical effects can be ignored ($d \gg \lambda$), and that the dielectric medium is irradiated from one side. While this front side faces air ($n_{\text{air}} = 1$) and has zero reflectivity (no primary reflection losses), the rear side is assumed to be ideally reflective. The light has to be fully randomized within the dielectric medium and the light scattering is assumed to be Lambertian (ideally diffuse). In case of a semiconductor material in which radiative recombination is the dominant recombination mechanism, the calculated absorption A_{Tiedje} can be compared to the QE of a solar cell. The model of Tiedje et al. provides an upper limit for the quantum efficiency since neither parasitic absorption nor primary reflection is considered.

In order to study these loss mechanisms in more detail, the work of Deckman and Wronski can be applied. Deckman and Wronski calculated a theoretical absorption probability F^{enh} using an infinite geometric progression [5]. Again, internal randomization and Lambertian light scattering are assumed. The sums of parasitic absorptions in the front contact and at the back reflector are given by A_{FC} and A_{BR}, respectively. Multiple reflections lead to an absorption in the silicon of

$$F^{\text{enh}} = \frac{1 - (A_{\text{FC}} + A_{\text{BR}})e^{-2\alpha d} - (1 - A_{\text{FC}} - A_{\text{BR}})e^{-4\alpha d}}{1 - (1 - A_{\text{FC}} - A_{\text{BR}})e^{-4\alpha d} + (1 - A_{\text{FC}} - A_{\text{BR}})n^{-2}e^{-4\alpha d}}. \quad (2)$$

3. Experimental results

First we reproduced two experimental results of previous studies [8,9], which are compared to calculations, and later utilized for optical-limitation estimations of thin-film silicon solar cells.

3.1. Front-contact ZnO:Al transpareny

Our standardly used ZnO:Al front contacts are deposited at a substrate temperature of 300 °C employing a ceramic target with 1 wt% Al_2O_3 target doping concentration (TDC). These films typically have a carrier concentration of $5 \times 10^{20}\,cm^{-3}$. Recent estimations have shown that a carrier concentration of about $2 \times 10^{20}\,cm^{-3}$ might optimally balance the optical and electrical needs [14]. By reducing the doping concentration of the sputter target, the carrier concentration can be controlled over a broad range [8,15]. A TDC of 0.5 wt% combined with a substrate temperature in the range of 350–380 °C has been identified as a promising combination of sputter-deposition parameters for ZnO:Al with optimized balance of conductivity, absorption and light-scattering properties [14].

Fig. 1 shows QE and total cell absorption $1-R_{\text{cell}}$ of a single junction p–i–n μc-Si:H solar cell with intrinsic silicon layer thickness of 1.0 μm. A reference front contact (dotted line, TDC = 1 wt%) and the optimized front contact with reduced carrier concentration (full line, TDC = 0.5 wt%) have been used. In the short-wavelength spectral range the QE is higher in the case of the reference front contact due to the Burstein–Moss effect [16,17]. Nevertheless, this effect is more than compensated for by the higher QE in the long-wavelength range in the case of the more transparent front contact with TDC = 0.5 wt% (full line). Altogether the corresponding cell-current density has been increased from 23.1 (reference) to $24.4\,mA/cm^2$ (TDC = 0.5 wt%). As other experiments have shown, even though the electrical conductivity of the front contact is reduced, the improved optical properties can lead to an overall higher conversion efficiency of solar modules [14].

3.1.1. Comparison with calculated absorptions

In order to consider a situation without light trapping, the absorption during two passes of a silicon layer of thickness d is calculated using

$$A_{\text{noLT}} = 1 - \exp(-2\alpha d). \quad (3)$$

This assumes no primary reflection losses and ideal reflectivity at the back contact, but no light scattering.

The theories summarized previously will be used in the following comparison to measure QEs of p-i-n thin-film silicon

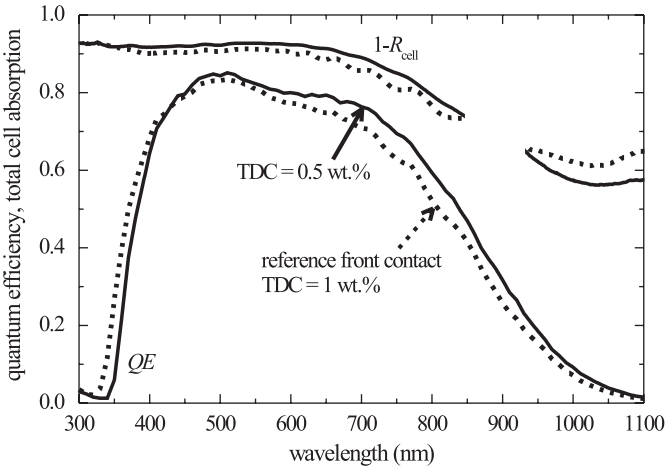

Fig. 1. Quantum efficiency (QE) and total cell absorption $1-R_{\text{cell}}$ of μc-Si:H single-junction cells (1.0 μm *i*-layer thickness) on reference ZnO:Al front contact with TDC = 1 wt% (dashed line) and more transparent front contact with TDC = 0.5 wt% (full line).

solar cells. To apply the theory of Deckman and Wronski, the front-contact absorption loss $A_{FC} = A_{TCO} + A_{p\text{-}Si}$ was expressed as the sum of absorption in the front-contact TCO and p-doped silicon layer. Accordingly, the back reflector losses $A_{BR} = A_{n\text{-}Si} + A_{ZnO/Ag}$ are given by the absorptions of the n-doped silicon and the back-reflector zinc oxide and silver. The spectral dependencies of A_{TCO}, $A_{p\text{-}Si}$, $A_{n\text{-}Si}$, $A_{ZnO/Ag}$ were determined by photothermal deflection spectroscopy (A_{TCO}, $A_{p\text{-}Si}$, $A_{n\text{-}Si}$) and transmission and reflection measurements using a spectrometer ($A_{ZnO/Ag}$). The layers used for optical characterization and the layers employed in solar cell experiments were nominally identical. To consider primary reflection losses R_{front} at the air/glass, glass/front contact and front contact/silicon interfaces as well as absorption losses in the front contact before entering the silicon for the first time, prefactors are taken into account. Thus, the calculated $QE_{Deckman}$ based on F^{enh} of Deckman and Wronski is given by

$$QE_{Deckman} = (1 - R_{front})(1 - A_{TCO})(1 - A_{p\text{-}Si})F^{enh}. \quad (4)$$

R_{front} is assumed to be 8% throughout the spectral range under consideration. Like in the publications of Tiedje et al. and Deckman and Wronski, the refractive index of the silicon layer n is assumed to be spectrally independent in the wavelength range of interest ($4n^2 = 50$). In reality, the refractive index of μc-Si:H typically varies from 3.8 to 3.5 in the spectral range of 600–1100 nm. In case of the glass substrate, the refractive index is almost constant at about 1.5 and it drops from 1.9 to 1.6 for the ZnO:Al front contact in the spectral range of 600–1100 nm. Note that the refractive indices of the glass substrate and the zinc oxide contact, for example, are not considered in the theory of Deckman and Wronski. In order to investigate the effect of the spectrally dependent refractive indices in more detail, more sophisticated computer simulation models like the ones presented by Vanecek et al. or Krc et al. have to be employed [18,19]. Nevertheless, calculations based on Eq. (4) reproduce the experimental results with high accuracy.

In Fig. 2, the aforementioned calculated absorptions are compared to an experimental QE (data already shown in Fig. 1, TDC = 0.5 wt%). While the absorption limit A_{Tiedje} exceeds the experimental data in the whole spectral range considerably, the calculation disregarding light trapping shows much lower absorption values in the long-wavelength range. The QE calculated using Eq. (4) based on the theory of Deckman and Wronski agrees closely with the experimental QE for nearly the entire spectral range of consideration. This calculation only shows observably higher values than in the experiment in the spectral range of 520–720 nm. The discrepancy is most likely due to the simplification in the model of Deckman and Wronski, which does not consider any index of refraction other than that of silicon (compare results shown in the following section).

3.2. Refractive-index matching interlayer at the front contact

Primary reflection can be reduced by refractive-index matching between adjacent layers. Therefore, a TiO_2 layer can be employed since the refractive index of TiO_2 is about 2.5 and thus between that of zinc oxide and silicon. It has already been shown experimentally that such a thin interlayer reduces reflection losses [6]. The TiO_2 thin-film deposition process has to be adjusted carefully to realize a transparent and sufficiently conductive film for the device application (for details see e.g. Ref. [9]). A chemical reduction of TiO_2, which will appear during the exposure to hydrogen plasma in PECVD deposition of microcrystalline silicon, leads to additional absorption losses. This can be prevented by a thin (approx. 10 nm thickness) coating of plasma-resistant ZnO on top of the TiO_2 layer [6]. Accordingly, a TiO_2/ZnO bilayer is used as an anti-reflection structure between the TCO front contact and silicon.

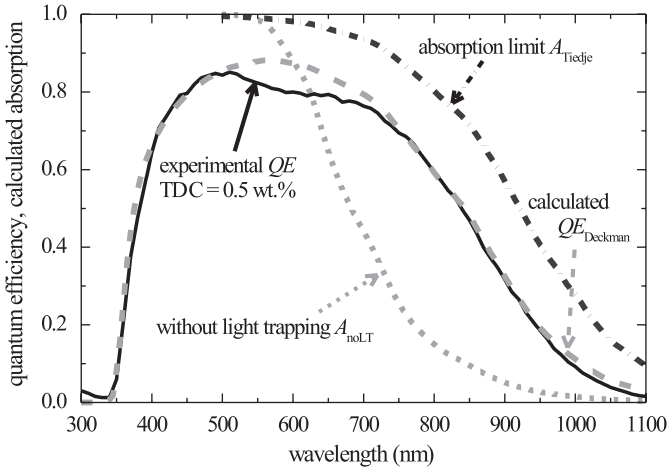

Fig. 2. Experimental quantum efficiency (QE) (full, black line, data for TDC = 0.5 wt% as already shown in Fig. 1, $j_{QE} = 24.4\,mA/cm^2$) in comparison to calculated absorptions based on theories by Tiedje et al. (dash–dotted, black line), Deckman and Wronski (dashed, gray line, $j_{QE} = 25.4\,mA/cm^2$) and without light trapping (dotted, gray line).

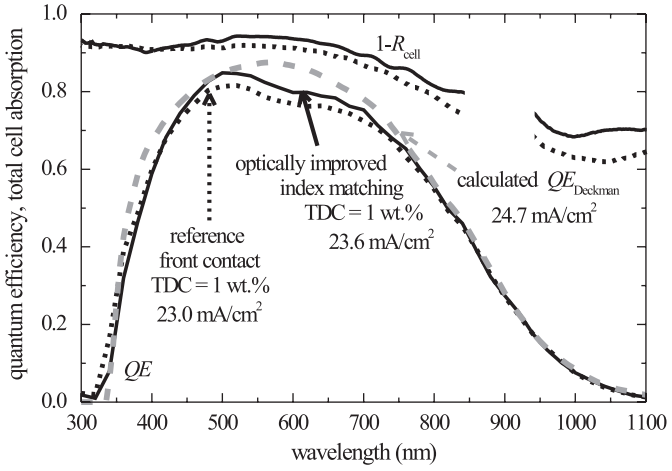

Fig. 3. QE and total cell absorption $1-R_{cell}$ of μc-Si:H single-junction cells (1.1 μm *i*-layer thickness) on reference ZnO:Al front contact with TDC = 1 wt% without (dashed line) and with refractive-index matching TiO_2 interlayer at the front contact (full line). For comparison, corresponding calculated $QE_{Deckman}$ values are shown (dashed, gray line).

In Fig. 3, QEs of simultaneously deposited μc-Si:H solar cells with intrinsic silicon layer thickness of 1.1 μm are shown. The application of a refractive-index matching interlayer at the front contact is compared to the reference case without TiO_2 layer. By introducing the TiO_2, the QE could be noticeably improved in the spectral range of 450–700 nm. In the long-wavelength spectral range, the parasitic absorption in the TiO_2 layer increases. This limits the positive effect of refractive-index matching [9]. The cell-current density was increased by $0.6\,mA/cm^2$. The total cell absorption $1-R_{cell}$ shows that the refractive-index matching layer reduced the reflection. It has been shown that this approach can lead to an overall increase in efficiency [20]. Again, like in Fig. 2, the calculated $QE_{Deckman}$ values are higher than the experimental QE in the intermediate spectral range. Nevertheless,

by introducing the refractive-index matching interlayer, the gap between the experimental values and $QE_{Deckman}$ could be reduced in the spectral range 500–700 nm. This indicates that the discrepancy between the experiment and the model might be mostly due to the simplification of considering only the absorption and not the refractive index of the different layers.

3.3. Optically improved back reflector

Surface-plasmon absorption is one of the parasitic absorption processes at the back reflector [21,22]. The spectral range of this absorption process depends on the refractive index of the medium directly attached to the silver. In order to improve the optical properties of the back reflector, an additional 50-nm-thick SiO_2 interlayer was introduced between back-contact ZnO and silver. In Fig. 4, the solar cell results compare the optical effect of the interlayer on QE and total cell absorption. The SiO_2 interlayer increased the QE in the spectral range of 540–900 nm, leading to an increase in cell-current density from 22.9 to 23.7 mA/cm^2 in the case of an intrinsic silicon layer thickness of 1.0 μm and a reference front contact with TDC = 1 wt%. The total cell absorption was reduced at the same time. Correspondingly, the gap between QE and total cell absorption shrank, indicating a lower level of parasitic absorption within the cell structure. Unfortunately, the gain in cell-current density did not increase the solar-cell efficiency. The fill factor decreased considerably due to deteriorated electrical properties. This problem is expected to be overcome by local contacts through the SiO_2 layer.

The experimental result, however, shows an optical improvement potential for the current density in the range of 0.8 mA/cm^2. This indicates the significance of the optical optimization potential at the back reflector. In order to consider the modified back reflector (ZnO/SiO_2/Ag) in calculations, the measured absorption of the ZnO/Ag-bilayer was employed. These data were rescaled for studying optical improvements. The experimentally realized increase in cell-current density could be reproduced in calculations both with respect to magnitude and—approximately—the spectral range of occurrence (not shown) by assuming a reduction of absorption to one-third of the value measured: $A_{BR} = A_{n\text{-}Si} + \frac{1}{3}(A_{ZnO/Ag})$.

4. Estimated optical limitations

4.1. Further potential of optical gain

The results presented so far show, that three individual optical improvements (reduced front contact absorption, refractive-index matching at the front contact and enhanced reflectivity of the back contact) increased the QE independently. The optical behavior of the cell could be described well by the calculations based on the theory of Deckman and Wronski. In the following section, further optical improvements will be studied. A cell with the improved front contact (target doping concentration 0.5 wt%, compare Fig. 1) is used as the reference for the calculations. For an estimation of optical losses we focus on the potential of QE gain by reducing different loss mechanisms to zero absorption. The absorption loss in each component depends on the loss in the other components, thus, we calculated the influence of an infinitesimally reduced loss of one cell component on the QE and extrapolated the gain in QE towards the case of zero absorption loss in the component under consideration. The results in case of a μc-Si:H single junction solar cell with intrinsic silicon layer thickness of 1.0 μm are indicated in Fig. 5. A cell-current density of 24.4 mA/cm^2 was achieved experimentally. The corresponding total cell absorption is shown as well (dashed line in Fig. 5). By reducing parasitic absorption in the front contact ZnO:Al, the QE is expected to increase up to the level indicated in Fig. 5. Correspondingly, by optical optimization of the front contact, the cell-current density can be increased by up to 2.7 mA/cm^2. Similarly, an optical optimization of the doped silicon layers (gray area in Fig. 5) is studied, indicating the most significant potential for a QE-increase in the spectral range 350–550 nm. The overall possible gain in cell-current density in the case of ideally transparent doped silicon layers is 1.4 mA/cm^2. A reduction of back-reflector absorption (black area) can increase the QE in the spectral range of $\lambda > 650$ nm significantly, offering a cell-current density potential of 2.0 mA/cm^2. The discrepancy between experimental data and calculated $QE_{Deckman}$ is most likely due to refractive-index mismatch. As it has been shown experimentally, the introduction of a refractive-index matching interlayer reduces the gap between experimental and calculated results. The overall potential of cell-current density increase by diminishing refractive-index mismatch reflection losses is 1.2 mA/cm^2, and this gain is expected primarily to be in the spectral range of 530–710 nm.

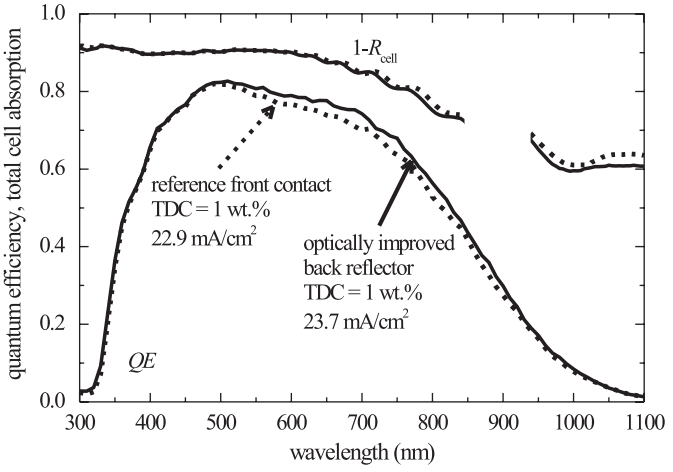

Fig. 4. QE and total cell absorption $1-R_{cell}$ of μc-Si:H single-junction cells (both with 1.0 μm *i*-layer thickness) on reference ZnO:Al front contact with TDC = 1 wt% without (dashed line) and with (full line) additional SiO_2 interlayer at back contact between ZnO and silver.

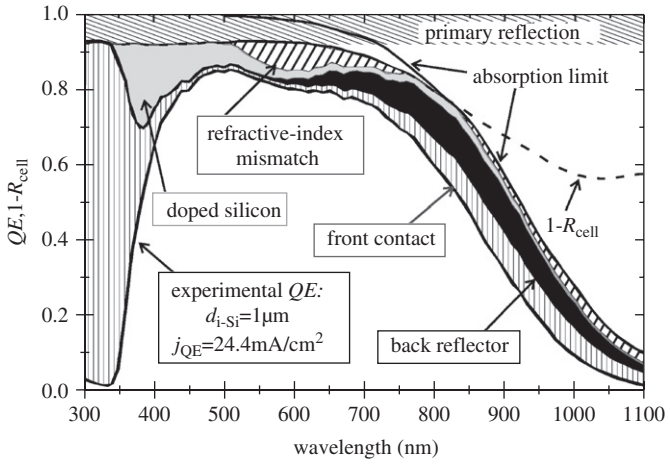

Fig. 5. QE and total cell absorption $1-R_{cell}$ of μc-Si:H single-junction cells (1.0 μm *i*-layer thickness) on more transparent ZnO:Al front contact with TDC = 0.5 wt% (same data as in Fig. 1) and estimated potential for QE increase in the case of reduced losses (details in the text).

In case of neither parasitic absorption losses nor refractive-index mismatch at any interfaces, the QE is expected to approach the level indicated as the absorption limit. For this idealized situation the theory of Deckman and Wronski and the calculations based on the model of Tiedje et al. using Eq. (1) lead to equal results. Additionally, the total cell absorption will be identical to the QE. Thus, it can be concluded that the gap between the absorption limit and the experimentally achieved total cell absorption (dashed line in Fig. 5) will not increase the QE by reducing parasitic losses. Due to the low absorption of a thin microcrystalline-silicon layer in the long-wavelength spectrum, the reflection losses are considerable: about 3.5 mA/cm^2 is lost due to primary reflection and 8.4 mA/cm^2 is lost due to secondary reflection. In order to overcome the absorption limitation indicated in Fig. 5, the light-trapping concept has to be modified. The light-scattering properties must be changed to lead to a deviation of the Lambertian angle distribution that traps the light even more efficiently. Possible systems to this purpose might be photonic crystals, nanoparticles, or up and down converters [23–26].

4.2. Outlook: combination of optical improvements

In this section, the combination of each optical improvement is studied by employing calculations based on the theory of Deckman and Wronski. Besides the already experimentally demonstrated optical improvements, the application of anti-reflection coating on the glass is assumed to reduce the primary reflection losses to only $R_{front} = 5.5\%$. For roughly estimating the resulting QE, we used the input parameters that were employed to reproduce the individual improvements within the model based on the theory of Deckman and Wronski. The results of this calculation are shown in Fig. 6. Accordingly, an increase of cell-current density from 24.4 to about 26.3 mA/cm^2 can be expected by combining the aforementioned improvements for a 1.0-μm-thick μc-Si:H single junction solar cell. The cell-current density depends on intrinsic silicon layer thickness strongly. This fact is considered in Fig. 7. It shows experimental results and estimations based on the assumptions in Fig. 6 of cell-current density in dependence on the intrinsic silicon layer thickness. A reference front contact with TDC of 1 wt% and an optimized front contact with TDC of 0.5 wt% are compared. Improving the front-contact transparency, the cell-current density can be increased by 1 to 1.7 mA/cm^2. Utilizing the other improvements, the resulting cell-current density level is still clearly below the absorption limit in the case of Lambertian light scattering as given by the calculation based on Tiedje et al. Nevertheless, these estimations show a cell-current density as high as 30 mA/cm^2 is already within reach. Only the previously experimentally demonstrated optical improvements (reduced front-contact absorption, improved refractive-index matching at the front contact and improved back-contact reflectivity) have been considered, combined with an anti-reflection coating of the glass substrate. Significant further potential is expected by improving the optical properties of the doped silicon layers [27].

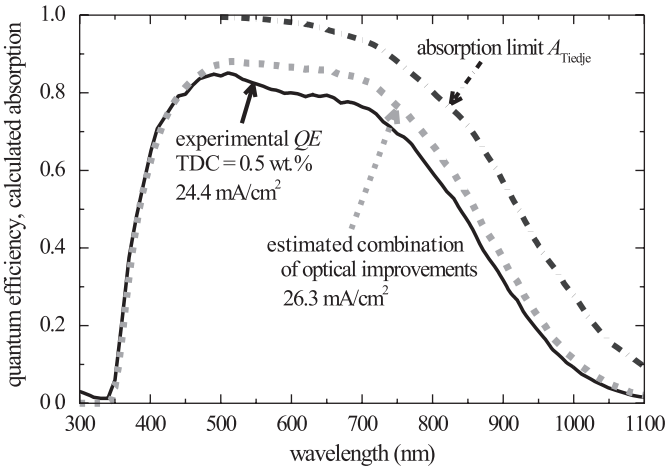

Fig. 6. Experimental QE (full, black line, data for TDC = 0.5 wt% as already shown in Figs. 1 and 2, intrinsic silicon layer thickness 1.0 μm) in comparison to calculated absorptions based on the theory by Tiedje et al. (dash–dotted, black line). The combination of optical improvements (details in the text) is studied using the theory of Deckman and Wronski (dashed, gray line).

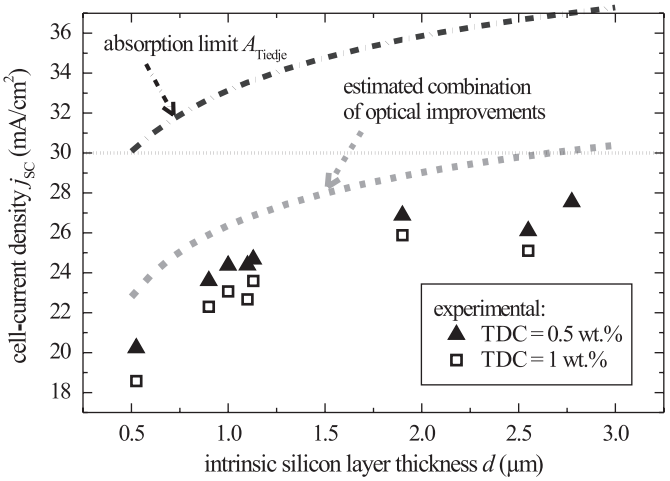

Fig. 7. Experimental cell-current density for reference front contacts (open square) and optimized front-contacts with improved transparency (full triangle). For comparison, calculated cell-current densities based on the absorption limit given by the theory of Tiedje et al. (dash–dotted line) and the calculations based on the theory of Deckman and Wronski, which assume a combination of individually proven optical improvements (dashed, gray line), are shown.

5. Conclusions

Improvements of QE and cell-current density of μc-Si:H solar cells were studied experimentally. An increase of front-contact ZnO:Al transparency, the application of a refractive-index matching interlayer at the front contact (TiO_2 between ZnO:Al and silicon) as well as an improved back-contact reflectivity (SiO_2 interlayer between back-contact ZnO and Ag) all individually demonstrated increased QE. Based on a model by Deckman and Wronski, the optical improvements could be reproduced in calculations. Further, calculations based on this model were employed to estimate the potential for optical improvements at different layers of the cell structure. Both front-contact transmission and back-contact reflectivity have the most significant potential for cell-current density increase.

The theory of Deckman and Wronski was applied to calculate a possible cell-current density by applying of the individual experimentally demonstrated optical improvements at the same time, combined with an additional anti-reflection coating of the glass substrate. Based on these assumptions, a cell-current density of more than 26 mA/cm^2 should be feasible for intrinsic silicon layer thickness of 1 μm. For thicker absorber layers, a cell-current density of 30 mA/cm^2 is already within reach.

Acknowledgments

The authors would like to thank A. Doumit, J. Kirchhoff, J. Klomfaß, G. Schöpe, and H. Siekmann for technical assistance,

and C. Das for helpful discussions. We gratefully acknowledge financial support from the Bundesministerium für Umwelt, Naturschutz und Reaktorsicherheit (German Federal Ministry for the Environment, Nature Conservation and Nuclear Safety) (contract no. 0329923 A) and the European Commission (Athlet project, contract no. 019670).

References

[1] S. Hegedus, Thin film solar modules: the low cost, high throughput and versatile alternative to Si wafers, Prog. Photovolt. Res. Appl. 14 (2006) 393.
[2] M.A. Green, Consolidation of thin-film photovoltaic technology: the coming decade of opportunity, Prog. Photovolt. Res. Appl. 14 (2006) 383.
[3] B. Rech, T. Repmann, M.N. van den Donker, M. Berginski, T. Kilper, J. Hüpkes, S. Calnan, H. Stiebig, S. Wieder, Challenges in microcrystalline silicon based solar cell technology, Thin Solid Films 511–512 (2006) 548.
[4] K. Yamamoto, A. Nakajima, M. Yoshimi, T. Sawada, S. Fukuda, T. Suezaki, M. Ichikawa, Y. Koi, M. Goto, T. Meguro, T. Matsuda, M. Kondo, T. Sasaki, Y. Tawada, High efficiency thin film silicon hybrid cell and module, in: Proceedings of the 15th International Photovoltaic Science & Engineering Conference, October, Shanghai, China, 2005, p. 529.
[5] H.W. Deckman, C.R. Wronski, Optically enhanced amorphous silicon solar cells, Appl. Phys. Lett. 42 (1983) 968.
[6] T. Matsui, T. Fujibayashi, A. Sato, H. Sonobe, M. Kondo, Improved spectral response of silicon thin film solar cells by TiO_2-ZnO antireflecting interbilayer at TCO/Si Interface, in: Proceedings of the 20th European PVSEC, 6–10 June, Barcelona, Spain, 2005, p. 1493.
[7] B. Rech, T. Roschek, T. Repmann, J. Müller, R. Schmitz, W. Appenzeller, Microcrystalline silicon for large area thin film solar cells, Thin Solid Films 427 (2003) 157.
[8] M. Berginski, J. Hüpkes, M. Schulte, G. Schöpe, H. Stiebig, B. Rech, M. Wuttig, The effect of front ZnO:Al surface texture and optical transparency on efficient light trapping in silicon thin-film solar cells, J. Appl. Phys. 101 (2007) 074903/01.
[9] M. Berginski, C. Das, A. Doumit, J. Hüpkes, B. Rech, M. Wuttig, Properties of TiO_2 layers as antireflection coating for amorphous silicon based thin-film solar cells, in: Proceedings of the 22nd EUPVSEC, September 3–7, Mailand, Italy, 2007, p. 2079.
[10] R. Carius, Photovoltaic and Photoactive Materials—Properties, Technology and Applications, vol. 93, Kluver Academic Publishers, 2002.
[11] E. Yablonovitch, G.D. Cody, Intensity enhancement in textured optical sheets for solar cells, IEEE Trans. Electron Devices ED 29 (1982) 300.
[12] E. Yablonovitch, Statistical ray optics, J. Opt. Soc. Am. 72 (1982) 899.
[13] T. Tiedje, E. Yablonovitch, G.D. Cody, B.G. Brooks, Limiting efficiency of silicon solar cells, IEEE Trans. Electron Devices 31 (1984) 711.
[14] M. Berginski, J. Hüpkes, W. Reetz, B. Rech, M. Wuttig, Recent development on surface-textured ZnO:Al films prepared by sputtering for thin-film solar cell application, Thin Solid Films, 2007, in press, doi:10.1016/j.tsf.2007.10.029.
[15] C. Agashe, O. Kluth, J. Hüpkes, U. Zastrow, B. Rech, M. Wuttig, Efforts to improve carrier mobility in radio frequency sputtered aluminum doped zinc oxide films, J. Appl. Phys. 95 (2004) 1911.
[16] E. Burstein, Anomalous optical absorption limit in InSb, Phys. Rev. 93 (1954) 632.
[17] T.S. Moss, The interpretation of the properties of indium antimonide, Proc. Phy. Soc. Lond. Sect. B 67 (1954) 775.
[18] J. Springer, A. Poruba, M. Vanecek, Improved three-dimensional optical model for thin-film silicon solar cells, J. Appl. Phys. 96 (2004) 5329.
[19] J. Krc, F. Smole, M. Topic, Analysis of light scattering in amorphous Si:H solar cells by a one-dimensional semi-coherent optical model, Prog. Photovolt. Res. Appl. 11 (2002) 15.
[20] C. Das, M. Berginski, J. Hüpkes, A. Gordijn, J. Kirchhoff, W. Reetz, A. Lambertz, F. Finger, W. Beyer, Improvement of short-circuit current in multijunction a-Si based solar cells using TiO_2 anti-reflection layer, in: Proceedings of the 22nd EUPVSEC, September 3–7, Mailand, Italy, 2007, p. 2112.
[21] E.A. Stern, R.A. Ferrell, Surface plasma oscillations of a degenerate electron gas, Phys. Rev. 120 (1960) 130.
[22] J. Springer, A. Poruba, L. Müllerova, M. Vanecek, O. Kluth, B. Rech, Absorption loss at nanorough silver back reflector of thin-film silicon solar cell, J. Appl. Phys. 95 (2004) 1427.
[23] E. Yablonovitch, Photonic band-gap structures, J. Opt. Soc. Am. B 10 (1993) 283.
[24] S. Pillai, K.R. Catchpole, T. Trupke, M.A. Green, Surface plasmon enhanced silicon solar cells, J. Appl. Phys. 101 (2007) 093105/1.
[25] T. Trupke, M.A. Green, P. Würfel, Improving solar cell efficiencies by up-conversion of sub-band-gap light, J. Appl. Phys. 92 (2002) 4117.
[26] T. Trupke, M.A. Green, P. Würfel, Improving solar cell efficiencies by down-conversion of high-energy photons, J. Appl. Phys. 92 (2002) 1668.
[27] Y. Huang, A. Dasgupta, A. Gordijn, F. Finger, R. Carius, Highly transparent microcrystalline silicon carbide grown with hot wire chemical vapor deposition as window layers in n–i–p microcrystalline silicon solar cells, Appl. Phys. Lett. 90 (2007) 203502/1.